

Research Paper

# The Structural Synthesis of Non-fractionated, Three-degree-of-freedom Planetary Gear Mechanisms

Sajad H. Abdali<sup>1</sup>, Essam L. Esmail<sup>2</sup>

Department of Mechanical Engineering, University of Al-Qadisiyah, Diwaniyah, 58001, Iraq, Email: eng.mech.4st-11@qu.edu.iq (S.H.A.); essam.esmail@qu.edu.iq (E.L.E.)

Received August 16 2023; Revised September 27 2023; Accepted for publication October 30 2023.

Corresponding author: E.L. Esmail (essam.esmail@qu.edu.iq)

© 2023 Published by Shahid Chamran University of Ahvaz

**Abstract.** Planetary gear trains (PGTs) with one or more degrees of freedom (DOFs) have numerous uses in PGT-based mechanisms. The majority of the currently available synthesis methods have focused on 1-DOF PGTs, with only a few investigations on multi-DOF PGT synthesis. The method for synthesizing 7-link 3-DOF PGMs is outlined. All possible link assortments are produced, labeled spanning trees are generated, and potential geared graphs are constructed. The guidelines for including geared edges and how to synthesize geared graphs are outlined. Vertex-degree arrays are generated to validate the geared graphs. Isomorphic geared graphs are identified by comparing the isomorphic identification numbers of geared graphs with the same spanning tree. Fractionated geared graphs are identified using the reachability matrix method. The new method has a straightforward algorithm. In contrast to what is reported in the literature, the results of the synthesis of 7-link 3-DOF PGMs show that there are seven non-fractionated mechanisms. MATLAB programs are used to acquire the vertex-degree arrays.

**Keywords:** Fractionated, Isomorphic, Link assortment, Planetary gear trains, Structural synthesis, Spanning tree.

## 1. Introduction

Planetary gear train (PGT) based mechanical equipment are extensively employed in vehicles transmissions, robot reduction devices, pulley blocks, machine and electrical equipment, robots, etc. The development of such equipment is heavily dependent on the development of planetary gear mechanisms (PGMs) [1-4]. PGTs are composed of central gears and planetary gears that revolve around them. Each pair of meshing gears is supported by a link known as the planet gear carrier, which keeps the distance between gear centers constant. Figure 1(a) depicts the functional schematic of the contra rotating gear train mechanism, whereas Fig. 1(b) depicts the related PGT graph. The contra rotating PGM is an eight-link three-DOF fractionated PGM comprised of a seven-link two-DOF fractionated PGT connected in series with its casing. The third degree of freedom is achieved simply by allowing the gear train to spin as a unit. A fractionated PGM has one or more separation links that can be broken into two or more parts to separate the PGM into distinct components. The basic structure of this mechanism is a seven-link two-DOF fractionated PGT, as shown in Fig. 1 (b).

Mechanism synthesis is easily handled by a computer when the structure of the mechanism can be defined by a topological graph and an adjacency matrix. PGT structure synthesis is a rapidly developing field in mechanism studies [5, 6].

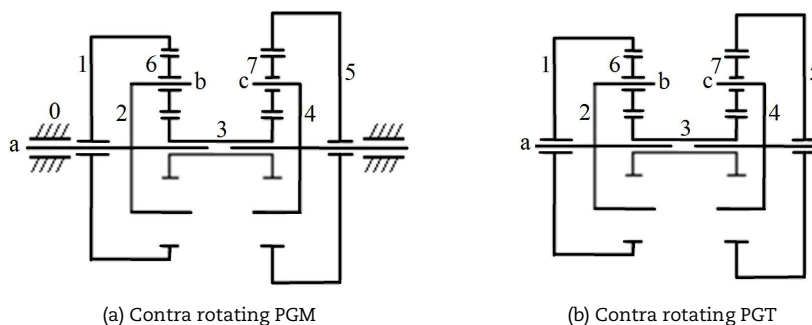


Fig. 1. The contra-rotating PGM and its PGT.



The vast majority of earlier synthesis methods [7–18] solely dealt with 1-DOF PGTs. The parent-graph-based approaches [15, 16, 19–22], recursive approaches [3, 7, 23, 24], acyclic-graph-based approaches [11, 25], and genetically compatible approaches [26] are fundamentally four unique approaches to the structural synthesis of PGTs. Shanmukhasundaram et al. [27] explored the majority of these approaches, whereas Xue et al. [28] investigated graph-based methods. Graph-based techniques may have issues with uniquely representing mechanisms. Graph-based approaches have also been applied to the study of two-degrees-of-freedom PGTs with up to nine links [29].

With the topology of a mechanism described by the topological graph and incidence matrix, the mechanism synthesis can be readily handled by a computer. Then it will be possible to automate the synthesis of mechanisms. A crucial step in the structural synthesis of PGMs is isomorphism determination; the accuracy of the isomorphism determination technique directly affects the quality of the results of the structural synthesis of PGMs. When two graphs are isomorphic, there is a one-to-one correspondence between each of the vertices and edges, preserving incidence. Detecting isomorphism in kinematic chains is a complex topic that has been studied for many years.

Methods to identify and remove isomorphic graphs were used during the synthesis of PGTs [10, 13, 15, 16, 17, 19, 20, 21, 29, 30, 31, 32]. Two graphs are said to be isomorphic if their edges and vertices maintain adjacency characteristics. Ravisankar and Mruthyunjaya [21] proposed an approach for detecting isomorphism in unlabeled graphs by employing adjacency matrix characteristic coefficients. Rao and Rao [13] identified isomorphic graphs using the Hamming matrix approach and the moment technique. Based on their prior perimeter-loop-based isomorphism identification approach, Yang and Ding [16, 30, 31] introduced a fully automated methodology for detecting isomorphic PGTs. Rai and Punjabi [32] described a simple link labeling approach that was utilized to identify a binary sequence that yields the largest binary code. To compare the isomorphism of PGTs, maxi codes are constructed, involving binary code and binary sequence. There are several empirical isomorphism testing methods that rely on a number of distinctive characteristics that, when combined, are sufficient to detect isomorphism [33–38]. However, there is a chance that structural isomorphism will go undetected. Counterexamples have been reported [39, 40].

Mruthyunjaya and Raghavan [41] introduced a matrix-based approach for analyzing kinematic chain structural characteristics. Ravishankar and Mruthyunjaya [42] proposed a completely computerized method for analyzing the structural properties of PGTs. Tsai [7] presented a method for synthesizing the topology of PGTs based on the linkage characteristic polynomial that uses random numbers. The graph-matrix algorithm was developed by Hsu and Lam [43] to analyze the kinematics of PGTs. Hsu [44] developed a novel approach to generating PGT graphs with up to seven links. He additionally established a straightforward approach for PGT structural synthesis. Hsu et al. [10] proposed an automated method for building PGT displacement graphs and employed structural code to detect graph isomorphism. Hsu [39] introduced a new graphical representation method for automatically generating displacement graphs for PGTs. Salgado and Castillo [45] used a computer program to generate all graphs with up to 9 links using the fundamental circuits of PGTs. Yang and Ding [16] developed the completed nine-link set of one-degree-of-freedom PGTs. Hsu et al. [43, 11] were the first to represent displacement graphs of PGTs using acyclic graphs. A portion of a connected graph with all of its edges having the same labels is represented as a polygon. In order to create displacement graphs from rotation graphs, Shanmukhasundaram et al. [17] suggested a new method based on kinematic units and acyclic graphs.

### 1.1. Scope and contributions

The goal of PGT structural synthesis is to create a catalog of all possible PGT topologies to aid designers in selecting the optimal topological structure for their PGT-based mechanisms.

Many multi-DOF PGTs can be created from a set of 1-DOF PGTs, but the former has received much less attention, and the literature on their synthesis results is inconsistent [16, 29]. Because the discrepancy in the results has yet to be resolved, the synthesis results are far from complete. No matter how many approaches to the topological synthesis of PGTs have been proposed, there is always the possibility of adopting new, simple methods for synthesizing PGTs that may produce different results. This paper describes a method for synthesizing 7-link 3-DOF PGMs (or 6-link 2-DOF PGTs).

A new method for synthesizing PGTs is devised by adding geared edges to spanning trees. The spanning trees of an N-link, F-DOF PGM are first counted using link assortment arrays. After that, the vertex degree arrays of the geared graphs are counted. The procedures for including geared edges and constructing geared graphs from spanning trees are described in detail, and geared graphs that contradict the vertex degree arrays are eliminated.

To detect isomorphic graphs, a method based on the weighted vertex degree array and the weighted vertex-circuit matrix is devised. The isomorphic identification numbers of geared graphs with the same spanning tree are compared to identify isomorphic geared graphs. If the isomorphic identification numbers of two graphs are the same, they are isomorphic.

The reachability matrix approach is used to identify fractionated geared graphs. Previous approaches to fractionated detection that rely on independent loop combinations varied greatly from the suggested method. The new approach is simple to implement and works for all potential graph representations.

Because other graph representations have difficulty adequately representing a PGM with multiple joints, the rooted graph (which matches to its mechanism) was employed in this work.

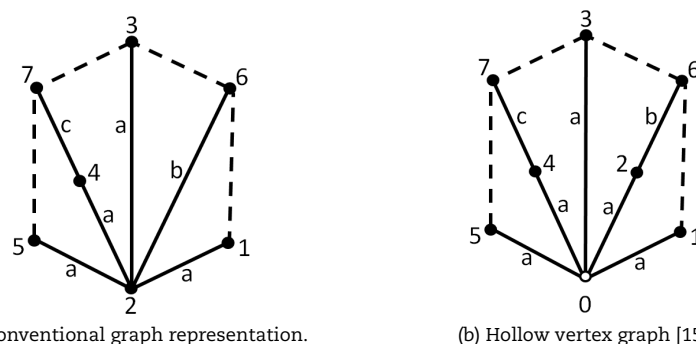


Fig. 2. Different graph representations of the contra-rotating PGM and its fractionation process.



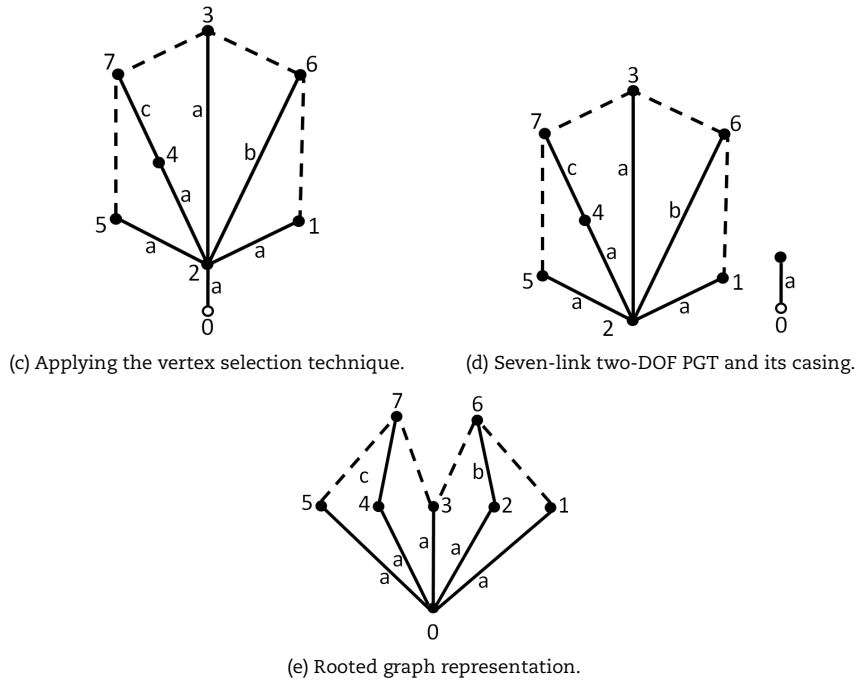


Fig. 2. Continued.

## 2. Preliminary Discussion to Graph Representation

### 2.1. Graph representation

According to the method created by Buchsbaum and Freudenstein [19], the conventional graph of the Contra rotating PGT can be represented as in Fig. 2(a). In graph representation, a vertex stands for a link and an edge stands for a joint. In this work, a revolute pair is represented by a thin edge and a geared pair is represented by a dashed edge. The conventional graph representation may lead to the generation of pseudo-isomorphic graphs [4, 15, 27, 38]. Pseudo-isomorphic graphs are those that are kinematically and functionally equivalent to their corresponding PGTs but are mathematically non-isomorphic. These PGTs are considered to be functionally isomorphic [5]. The detection of isomorphism will be greatly complicated or prone to errors if there are pseudo-isomorphic graphs present. As a result, whenever possible, such graphs should be avoided.

Yang et al. [15] represented the structure of PGTs by using a new graph model with solid and hollow vertices. Hollow vertices represent multiple revolute joints on the same level. Therefore, PGTs with revolute joints of different levels only have solid vertices. The graph representation in accordance with the method of Yang et al. [15] is shown in Fig. 2(b). For this graph representation model, there are two different types of graphs: graphs with one or more hollow vertices and graphs without a hollow vertex. Since the vertices represent the links, the number of vertices should not exceed the number of links. In a hollow vertex graph, the number of vertices exceeds the number of links; hence, there is no one-to-one correspondence with the PGT. The graph in Fig. 2(b) has the following adjacency matrix:

$$A = \begin{bmatrix} & v_0 & v_1 & v_2 & v_3 & v_4 & v_5 & \vdots & v_6 & v_7 \\ v_0 & 0 & 1 & 1 & 1 & 1 & 1 & \vdots & 0 & 0 \\ v_1 & 1 & 0 & 0 & 0 & 0 & 0 & \vdots & 1 & 0 \\ v_2 & 1 & 0 & 0 & 0 & 0 & 0 & \vdots & 1 & 0 \\ v_3 & 1 & 0 & 0 & 0 & 0 & 0 & \vdots & 1 & 1 \\ v_4 & 1 & 0 & 0 & 0 & 0 & 0 & \vdots & 0 & 1 \\ v_5 & 1 & 0 & 0 & 0 & 0 & 0 & \vdots & 0 & 1 \\ \dots & \vdots & \dots & \dots \\ v_6 & 0 & 1 & 1 & 1 & 0 & 0 & \vdots & 0 & 0 \\ v_7 & 0 & 0 & 0 & 1 & 1 & 1 & \vdots & 0 & 0 \end{bmatrix} \quad (1)$$

Links 1, 2, 3, 4, and 5 in the graph depicted in Fig. 2 (b) share a common joint axis, "a". Vertex selection is the act of changing a revolute edge with one that is of the same level [5]. Figure 2(c) illustrates how the vertex selection approach can be used to rearrange the graph in order to check for a cut vertex. Figure 2(d) reveals a cut vertex, indicating that the graph represents a 3-DOF PGM with fractional DOF. The formula for the degree of freedom (F) of a v-vertex graph is:

$$F = 3 \times (v - 1) - 2 \times e_r - 1 \times e_g \quad (2)$$

where the number of revolute edges is denoted by  $e_r = v - 1$  and the number of geared edges is denoted by  $e_g = v - 1 - F$ .

For the Contra rotating PGM shown in Fig. 2(b), we have  $v = 8$  and  $e_r = 7, e_g = 4$ . Equation (2) gives  $F = 3(8 - 1) - 2 \times 7 - 4 = 3$ . For the PGT shown in Fig. 2(a), we have  $v = 7$  and  $e_r = 6, e_g = 4$ . Equation (2) gives  $F = 3(7 - 1) - 2 \times 6 - 4 = 2$ . Figure 2(d) shows the graphs of the contra rotating PGT and its casing. Therefore, it is a fractionated 3-DOF PGM. It consists of a 2-DOF PGT that is held up by the frame on a central axis. However, this graph model has trouble accurately modeling a PGM containing multiple joints. This necessitated the use of a graph that is consistent with its mechanism, called the rooted graph. The vertex that represents the frame of a mechanism is referred to as the root in a rooted graph representation. Because at least one link in the PGT has its geometric axis rotated around the fixed axis of the mechanism, all graphs must have a root. Figure 2(e) shows the rooted graph for the contra rotating PGM. Vertex 0 is the root.



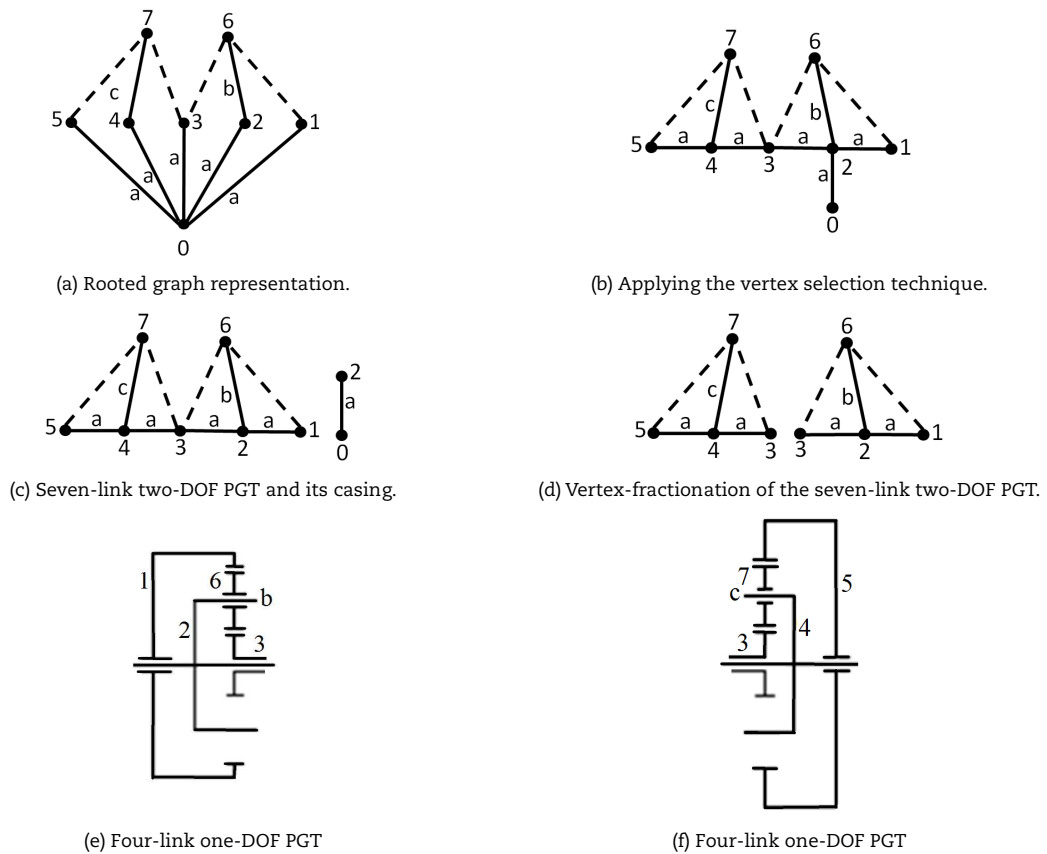


Fig. 3. Rooted graph representation of the contra-rotating PGM and its fractionation process.

2.2. Fractionated graphs

A fractionated mechanism consists of two kinematic chains that share either a common joint but no common link or a common link but no common joint. A cut vertex is a vertex in a graph that, when removed, creates more subgraphs. If, after applying vertex selection once or more times, one of the pseudo isomorphic graphs of a given kinematic chain has one or more cut vertices, we say that the graph is fractionated. However, there can be as many as  $\binom{m}{m-2}$  pseudoisomorphic graphs in a graph with  $m$  vertices connected by revolute edges of the same edge level. As the number of edges sharing a common edge level grows, it becomes more challenging to derive all the pseudo isomorphic graphs.

The graph in Fig. 3(a) can be reconfigured using the vertex selection technique to become one with a separating vertex, as seen in Fig. 3(b). A cut vertex is a vertex in a graph whose removal, in conjunction with the removal of incident edges, yields a graph with more components than the original [5, 15]. If a graph is connected and has no cut vertices, it is referred to as a block. The separating vertex that can divide the graph into two sub-graphs is vertex 2 as shown in Fig. 3(c). This mechanism is a typical fractionated one in that links 1, 2, 3, 4, 5, 6, and 7 together contribute to making a 2-DOF gear train. The third degree of freedom is made possible by the PGT's ability to spin as a unit about axis "a," which represents the fixed link 0.

Also, vertex 3 is a separation vertex in the 2-DOF PGT. The separating link that can divide the seven-link two-DOF PGT into two four-link one-DOF PGTs is link 3 as shown in Figs. 3(d) and (f).

Despite the advantages, fractionated PGTs are often synthesized by splitting larger PGTs down into their fractionated parts with a reduced degree of freedom. It is quite simple and is not the subject of this study. When working on the synthesis of higher-degree-of-freedom PGTs, it is important to identify and get rid of any fractionated PGTs. Here, we introduce a straightforward new technique for identifying fractionated PGT graphs. Previous techniques relied on rotation graphs rather than displacement graphs to detect fractionation. When the graph of a fractionated PGT is transformed into a rotation graph, the cut vertex is the one whose removal results in a larger number of components. The new method relies on the successive deletion of revolute joints with the same labeling from the geared graphs. A graph is considered to be fractionated if at least one of its resulting sub-graphs is also fractionated with a larger number of components using a single application of upper-level vertex separation.

2.3. Correspondence between PGMs and rooted graphs

Because a PGM's structure may be expressed as a graph, a number of desired graph characteristics can be transformed into PGM characteristics.

Assume  $J_r$  represents the number of revolute joints and  $J_g$  represents the number of gear joints. Because gear joints have two degrees of freedom and revolute joints have one degree of freedom, the total number of joints is given by:

$$J = J_g + J_r \tag{3}$$

The degrees of freedom as a whole can be expressed as:

$$\sum_{i=1}^j f_i = 2J_r + J_g \tag{4}$$



where  $f_i$  denote the DOF in the  $i^{th}$  joint. Therefore, an n-link PGM has an overall DOF of:

$$DoF = 3(n - 1) - 2J_r - J_g \tag{5}$$

An important consideration for geared kinematic chains is that the number of gear joints is always less than that of revolute joints and it is based on the following inequality:

$$J_r \geq J_g + 1 \tag{6}$$

Since an n-link PGM has  $v$  vertices in its rooted graph, and the revolute edges are always in the shape of a tree, therefore the number of revolute edges is limited by the following equation:

$$e_r = v - 1 \tag{7}$$

And the number of revolute joints is:

$$J_r = n - 1 \tag{8}$$

Consequently, a PGM's overall number of joints should equal:

$$J = J_r + J_g \tag{9}$$

Since each edge in the rooted graph represents a joint, the sum of the revolute edges  $e_r$  and the geared edges  $e_g$  equals the number of joints in the PGM:

$$e = e_r + e_g = J \tag{10}$$

Eq. (5) can be rewritten using the number of vertices and edges as:

$$DoF = 3(v - 1) - (2e_r + e_g) \tag{11}$$

Substituting Equations (7) and (10) into Eq. (11) yields:

$$DoF = 2v - e - 2 \tag{12}$$

Substituting Eq. (7) into Eq. (11), simplifying and arranging yields:

$$e_g = v - 1 - DoF \tag{13}$$

Therefore, an n-DoF, n-link PGM has a graph with  $(e_r - F)$  geared edges.

The number of vertices, edges, and independent loops in a planar-connected graph are all governed by Euler's equation, which may be expressed as:

$$L = e - v + 1 \tag{14}$$

Substituting Eq. (7) into Eq. (10), we obtain:

$$e_g = e - v + 1 \tag{15}$$

Substituting Equations (7) and (15) into Eq. (10) yields:

$$DoF = e_r - e_g \tag{16}$$

The correspondence between the constituents of a PGM and those of a rooted graph is summarized in Table 1. The PGM and its rooted graph representation have a one-to-one correspondence.

### 3. Basic Introductory Concepts

#### 3.1. Characteristics of planetary gear mechanisms

A PGM is defined as a geared kinematic chain containing only revolute and geared joints [5]. A PGM is a  $(f+1)$ -DOF fractionated mechanism. It is made up of an f-DOF PGT, with the mechanism's housing supporting its center axis. Since the complete PGT can be rotated around its central axis, this provides an additional degree of freedom. A PGM must confirm to the following rules:

1. The casing is connected to the PGT through revolute joints.
2. The PGM shall obey the general degrees of freedom equation (Eq. (2)).
3. On the axis of each gear, there must be a revolute joint.
4. A carrier is located between each gear pair to maintain a constant distance between the two gears.
5. There cannot be any partial mobility; each link must be capable of unlimited rotation.

**Table 1.** The numerical correspondence relationship between PGMs and their rooted graphs.

Rooted Graphs	Symbol	PGMs	Symbol
Vertices	v	Links	n
Edges	e	Joints	J
Revolute edges	$e_r$	Revolute joints	$J_r$
Geared edges	$e_g$	Geared joints	$J_g$
Vertices of degree i	$v_i$	Links having i joints	$n_i$
Degree of vertex i	$d_i$	Joints on link i	$d_i$
Independent loops	L	Independent loops	L
Total loops (L + 1)	$\tilde{L}$	Total loops (L + 1)	$\tilde{L}$



### 3.2. Fundamental characteristics of the graphs of PGMs

The graph of a PGM of ( $n$ ) links possess the following characteristics [5, 26]:

- C1. The graph has ( $v$ ) vertices and ( $v - 1$ ) revolute edges.
- C2. The number of geared edges equals the difference between the number of revolute edges and the DOF of the PGM.
- C3. A spanning tree is obtained by removing all of the gear edges from the graph.
- C4. Any geared edge added to the spanning tree creates a fundamental circuit with one geared edge and multiple revolute edges.
- C5. The total number of fundamental circuits is equal to the total number of geared edges.
- C6. The revolute edges are labeled based on where their axes are in space.
- C7. A tree must be formed by all revolute edges with the same label.
- C8. There is one vertex in each fundamental circuit called the transfer vertex; all edges on one side of the transfer vertex have the same label, while edges on the opposite side of the transfer vertex have a different label.

### 3.3. Isomorphic identification methodology

#### 3.3.1. Vertex degree string for spanning trees

Using the rooted graph, it is possible to differentiate explicitly the similarities and differences between numerous PGMs. Specifically, the vertices may be subdivided into many levels. The root is located at the ground level. First-level vertex refers to a vertex that has a direct connection to the root by a single revolute edge. If a vertex has two revolute edges connecting it to its root, it is considered to be of the second level. This may be repeated on subsequent levels, if applicable. Vertex levels are shown in Fig. 4: vertex 0 is on the ground level, vertices 1, 2, and 3 are on the first level, vertices 4, and 5 are on the second level, and vertex 6 is on the third level.

Graphs may be classified into families based on their spanning trees. Graphs from distinct families cannot be isomorphic. Two graphs with different spanning trees are not isomorphic. The degree of a vertex  $i$ , denoted by  $d_i$ , is the number of edges that are incident with it. The vertex degree string is used to classify spanning trees. It is defined as an ascending sequence of numbers denoting the degree of vertices beginning from ground level. In particular, the first number in the vertex degree string denotes the degree of the ground vertex, the second denotes the degree of the vertex with the highest vertex degree in the first level, and so on. For example, the spanning tree shown in Fig. 4 (b) has a vertex degree string of 3:311:21:1.

The first step in identifying isomorphism is to classify graphs depending on their VDSs. Isomorphism is not possible in graphs with different VDSs. The required condition for testing graph isomorphism is provided by the VDSs of spanning trees. When there is no one-to-one correspondence between the vertices of two graphs, we say that they are not isomorphic, and we test this by comparing their correspondence.

Figure 5 depicts two rooted graphs with seven links and nine edges. Figure 5(a) shows the vertices extending to the third level, while Fig. 5(b) shows the vertices reaching the second level. Hence, their spanning trees have VDSs of 3:311:21:1 and 3:321:111, respectively. Therefore, they are not isomorphic.

#### 3.3.2. Isomorphic identification number

The number of edges that are incident with a vertex  $i$  is referred to as its degree, and it is represented by the notation  $d_i$ . In the graph depicted in Fig. 5(a), the degree of the vertices numbered 0, 1, 4, and 5 is three, whereas the degree of the vertices numbered 2, 3, and 6 is two. In mathematical expression,  $d_0 = 3, d_1 = 3, d_2 = 2, d_3 = 2, d_4 = 3, d_5 = 3,$  and  $d_6 = 2$ .

The vertex degrees of the vertices of a graph can be used to classify the vertices of the graph. The vertex degree array (VDA) is a set of numbers that collectively indicate the degrees of the vertices. These numbers are denoted by the following notation:  $[d_0, d_1, d_2, \dots, d_{v-1}]$ .

$$D = [d_0, d_1, d_2, \dots, d_{v-1}] \tag{17}$$

The VDA for Fig. 4(a) can be written down as [3 3 2 2 3 3 2].

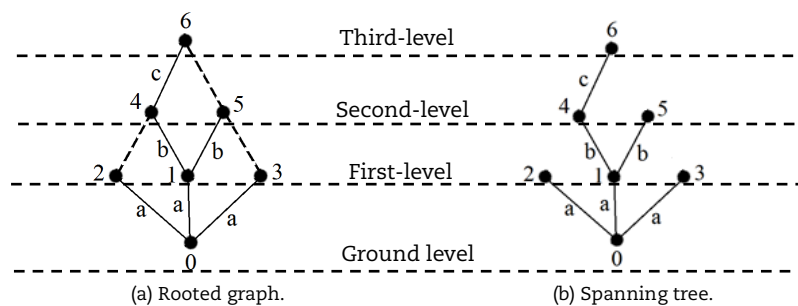


Fig. 4. Vertex levels.

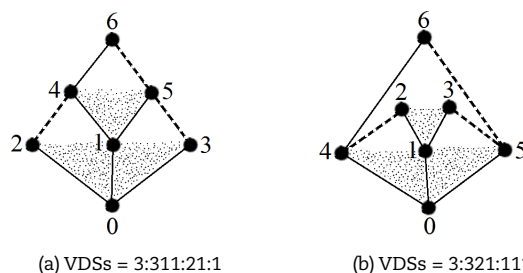


Fig. 5. VDSs of Two rooted graphs with seven links and nine edges.





The circuit degree string is,  $CDS = 66595957$ .  
 The isomorphic identification number is:

$$(IIN)_a = 34112111666595957 \tag{23}$$

Similarly,

$$(FCAA)_b = [3 \ 3 \ 4 \ 3 \ 4 \ 5 \ 5 \ 3] \begin{bmatrix} 3 & 3 & 0 & 0 \\ 3 & 0 & 0 & 0 \\ 4 & 4 & 4 & 4 \\ 0 & 3 & 0 & 0 \\ 4 & 0 & 0 & 4 \\ 0 & 0 & 5 & 5 \\ 0 & 5 & 5 & 0 \\ 0 & 0 & 0 & 3 \end{bmatrix} = \begin{bmatrix} 50 \\ 59 \\ 66 \\ 66 \end{bmatrix} \tag{24}$$

Therefore,  $(IIN)_b = 3411211166665950 \neq (IIN)_a$ . Since  $(IIN)_a \neq (IIN)_b$ , the two graphs shown in Fig. 6 are non-isomorphic.

### 4. Fractionated Graph Detection

#### 4.1. Reachability Matrix

The reachability matrix (RM) can be used to determine whether a path exists in a graph between any two vertices. The  $(i, j)^{th}$  entry in the RM of a  $v$ -vertex graph has the value 1 if there is a path from  $v_i$  to  $v_j$  and 0 otherwise. Therefore, the reachability matrix can be written as a  $v \times v$  zero-one matrix as following:

$$rm(i, j) = \begin{cases} 1 & \text{if there is a path from vertex } v_i \text{ to vertex } v_j \\ 0 & \text{otherwise} \end{cases} \tag{25}$$

Each entry  $rm(i, i)$  is one since every  $v_i$  has a path to itself.

The number of different paths of length  $v$  from  $v_i$  to  $v_j$ , equals the  $(i, j)^{th}$  entry  $[a(i, j)]^v$  of  $(A)^v$  where  $A$  is the adjacency matrix of the graph. The reachability matrix is the logical matrix of  $(\tilde{A} + I)^{v-1}$  where  $\tilde{A}$  is the reduced adjacency matrix and  $I$  is the identity matrix. The new technique is not concerned with the actual number of paths of length  $(v - 1)$  in the graph; rather, it is concerned with whether or not a path exists.

#### 4.2. The fractionated detection algorithm

To determine whether a PGT is non-fractionated, we first remove the revolute joints with the same labeling and separate the upper-level vertices connected to them individually. A PGT is said to be fractionated if at least one of its resulting sub-graphs is also fractionated. This acts as the foundation for the subsequent detection algorithm.

**Step 1:** Create a graph for the given PGT.

**Step 2:** Generate a sub-graph by deleting the root vertex. When a vertex is removed, all the edges that are incident to it are also removed.

**Step 3:** Among the vertices that are incident by the deleted edges, check for the presence of a vertex having a degree of at least two. It is obvious that a separation link has to be at least a binary link or the cut vertex must have a degree of at least two. If the graph has no such vertex, then it cannot be fractionated. If there is at least one such vertex, you can move on to the next step.

**Step 4:** Remove one of the vertices with a degree of two or higher.

**Step 5:** Check if there are two sub-graphs or more, then, the graph is fractionated and there is no need for additional verification. If not proceed to the next step.

**Step 6:** Repeat step 3 by choosing a different vertex as many times as needed. If no cut vertex is detected, proceed to the next step.

**Step 7:** Delete another group of revolute joints with the same labeling from the original graph. Then, repeat step 3 until all groups are examined.

The fractionated detection algorithm can be visualized graphically as shown in Fig. 7.

By eliminating the root vertex, we obtain the graph depicted in Fig. 7(b). The three vertices that are incident by the removed edges in Fig. 7(b) are  $v_1, v_2$ , and  $v_3$ , with vertex 1 having a degree of 3. Figure 7(c) is the result of removing vertex 1. Because Fig. 7(c) has two sub-graphs, the graph is fractionated, and vertex 1 is the cut vertex.

#### 4.3. Computer implementation

The adjacency matrix for the graph represented in Fig. 7(a) is as follows:

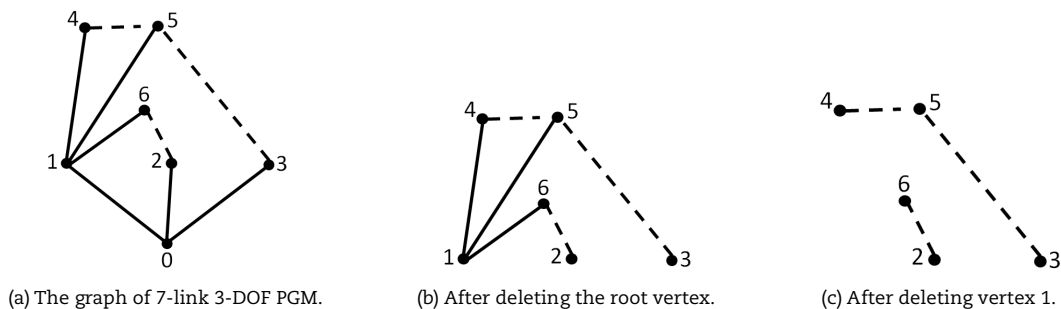


Fig. 7. The fractionation process of 7-link 3-DOF PGM.



$$A = \begin{bmatrix} & v_0 & v_1 & v_2 & v_3 & \vdots & v_4 & v_5 & v_6 \\ v_0 & 0 & 1 & 1 & 1 & \vdots & 0 & 0 & 0 \\ v_1 & 1 & 0 & 0 & 0 & \vdots & 1 & 1 & 1 \\ v_2 & 1 & 0 & 0 & 0 & \vdots & 0 & 0 & 1 \\ v_3 & 1 & 0 & 0 & 0 & \vdots & 0 & 1 & 0 \\ \dots & \dots & \dots & \dots & \dots & \vdots & \dots & \dots & \dots \\ v_4 & 0 & 1 & 0 & 0 & \vdots & 0 & 1 & 0 \\ v_5 & 0 & 1 & 0 & 1 & \vdots & 1 & 0 & 0 \\ v_6 & 0 & 1 & 1 & 0 & \vdots & 0 & 0 & 0 \end{bmatrix} \tag{26}$$

The reduced adjacency matrix is obtained by deleting row 1 and column 1:

$$\tilde{A} = \begin{bmatrix} & v_1 & v_2 & v_3 & \vdots & v_4 & v_5 & v_6 \\ v_1 & 0 & 0 & 0 & \vdots & 1 & 1 & 1 \\ v_2 & 0 & 0 & 0 & \vdots & 0 & 0 & 1 \\ v_3 & 0 & 0 & 0 & \vdots & 0 & 1 & 0 \\ \dots & \dots & \dots & \dots & \vdots & \dots & \dots & \dots \\ v_4 & 1 & 0 & 0 & \vdots & 0 & 1 & 0 \\ v_5 & 1 & 0 & 1 & \vdots & 1 & 0 & 0 \\ v_6 & 1 & 1 & 0 & \vdots & 0 & 0 & 0 \end{bmatrix} \tag{27}$$

The three vertices that are incident by the removed edges are  $v_1, v_2, v_3$ , and vertex 1 has a degree more than 2. By removing vertex 1, we get the matrix  $\tilde{A}_{-v_1}$ . The  $(\tilde{A}_{-v_1} + I)$  matrix is then obtained, where I is the identity matrix. The identity matrix is added since every vertex has a path to itself:

$$\tilde{A}_{-v_1} + I = \begin{bmatrix} & v_2 & v_3 & \vdots & v_4 & v_5 & v_6 \\ v_2 & 1 & 0 & \vdots & 0 & 0 & 1 \\ v_3 & 0 & 1 & \vdots & 0 & 1 & 0 \\ \dots & \dots & \dots & \vdots & \dots & \dots & \dots \\ v_4 & 0 & 0 & \vdots & 1 & 1 & 0 \\ v_5 & 0 & 1 & \vdots & 1 & 1 & 0 \\ v_6 & 1 & 0 & \vdots & 0 & 0 & 1 \end{bmatrix} \tag{28}$$

and,

$$(\tilde{A}_{-v_1} + I)^{v-1} = \begin{bmatrix} & v_2 & v_3 & \vdots & v_4 & v_5 & v_6 \\ v_2 & 16 & 0 & \vdots & 0 & 0 & 16 \\ v_3 & 0 & 21 & \vdots & 20 & 29 & 0 \\ \dots & \dots & \dots & \vdots & \dots & \dots & \dots \\ v_4 & 0 & 20 & \vdots & 21 & 29 & 0 \\ v_5 & 0 & 29 & \vdots & 29 & 41 & 0 \\ v_6 & 16 & 0 & \vdots & 0 & 0 & 16 \end{bmatrix} \tag{29}$$

The reachability matrix is the logical matrix of  $(\tilde{A}_{-v_1} + I)^{v-1}$  and can be calculated by using a MATLAB program as:

$$RM = \begin{bmatrix} 1 & 0 & 0 & 0 & 1 \\ 0 & 1 & 1 & 1 & 0 \\ 0 & 1 & 1 & 1 & 0 \\ 0 & 1 & 1 & 1 & 0 \\ 1 & 0 & 0 & 0 & 1 \end{bmatrix} \tag{30}$$

The presence of zeroes in RM after removing vertex 1 shows the existence of a cut vertex, which disconnects the graph.

### 5. Systematic Synthesis Methodology

To construct all n-link 3-DOF PGM graphs, simply add  $n - 4$  geared edge to each  $n$ -vertex spanning tree, as specified by the fundamental rules. The following is a brief summary of a systematic approach to the structural synthesis of n-link 3-DOF PGMs:

1. List all  $n$ -vertex spanning trees.
2. Enumerate the different  $n$ -vertex geared graphs that can be created from each spanning tree via the addition of  $n - 4$  geared edges.
3. Nevertheless, there is a possibility that some of the synthesized graphs will not meet the required fundamental characteristics C1-C8. Graphs with gears that don't adhere to the fundamental characteristics should be eliminated.
4. If two geared graphs share the same spanning tree, but have distinct isomorphic identification numbers, then the graphs are not isomorphic. It is correct that geared graphs synthesized from distinct sets of spanning trees do not share any common properties.
5. All  $n$ -vertex spanning trees must be employed, therefore repeat Steps 2-4 until that happens.
6. Determine the fractionated PGTs and eliminate them to complete the catalog of  $n$ -link three-DOF PGM graphs.

Synthesis of non-fractionated 3-DOF PGMs with non-isomorphic structures is performed based on an atlas of spanning trees. The main objective of PGM synthesizing is to produce all possible geared graphs. Each geared graph correlates to a certain topology and function of a PGM. Figure 8 depicts the flowchart of the synthesis process.

#### 5.1. Synthesis of spanning trees

The revolute edges can be represented by a spanning tree. The spanning tree for the graph displayed in Fig. 4 is shown in Fig. 9. The axes' positions in space are denoted a, b, and c. However, same-level revolute edges are generally known to be identical to multiple-joint [5, 15, 25, 44].

In the new graph representation, the edges of identical labels that are incident to the same vertex are denoted by a dotted polyline. Figure 9(b) shows a dotted polyline spanning tree. The number of distinct labels is equal to the number of single edges and/or dotted polylines, which is a major benefit of using a dotted polyline spanning tree.



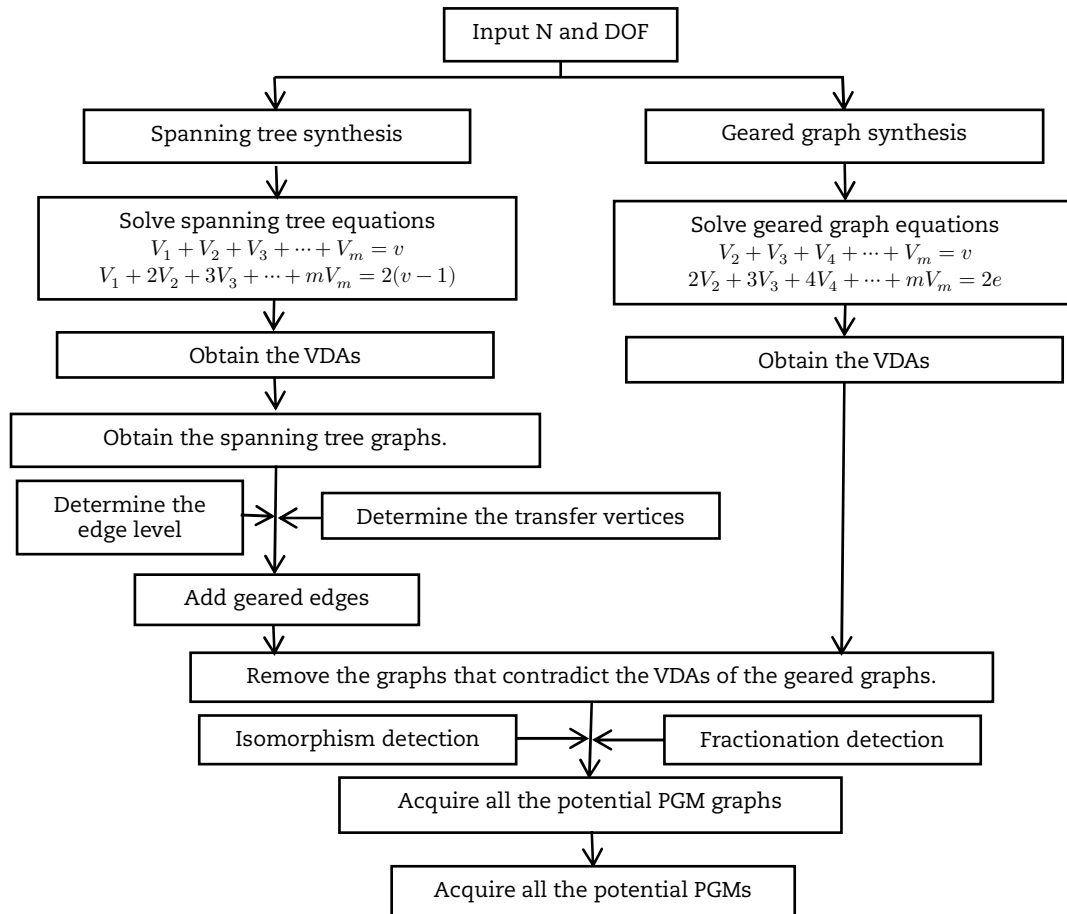


Fig. 8. Flowchart for the synthesis process.

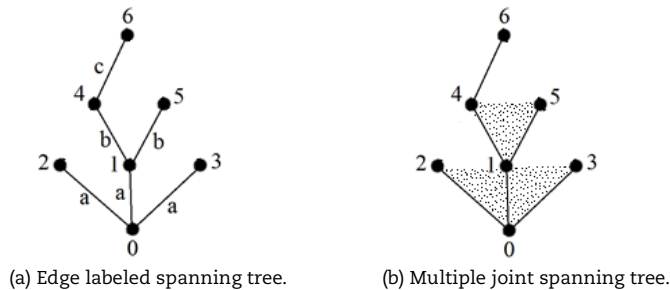


Fig. 9. The spanning tree for the graph displayed in Fig. 4(a).

The link assortment array of a spanning tree is written as  $[V_1, V_2, V_3, \dots, V_m]$ , where  $V_1, V_2, V_3, \dots, V_m$  are the numbers of vertices of degree one, two, there, ...,  $m$ , respectively. The parameter  $m$  is the maximal vertex degree in a graph and is calculated by the following equation.  $m = L + 1 = n - F$ . All possible link assortments of spanning trees satisfy the following two equations:

$$V_1 + V_2 + V_3 + \dots + V_m = v \tag{31}$$

$$V_1 + 2V_2 + 3V_3 + \dots + mV_m = 2(v-1) \tag{32}$$

Consider the spanning trees of seven-link three-DOF PGMs, with  $v = 7, F = 3$ , and  $m = 7 - 3 = 4$ . We obtain from Eqs. (31) and (32):

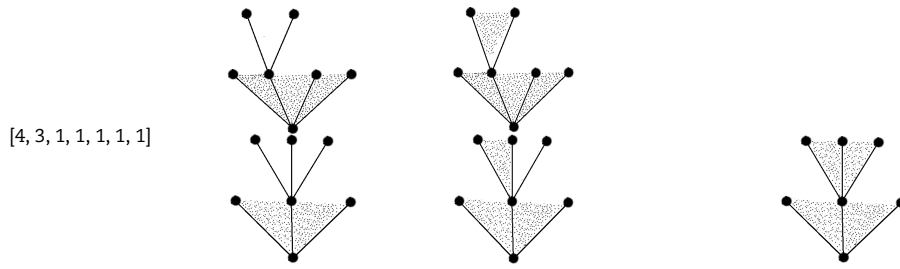
$$V_1 + V_2 + V_3 + V_4 = 7 \tag{33}$$

$$V_1 + 2V_2 + 3V_3 + 4V_4 = 12 \tag{34}$$

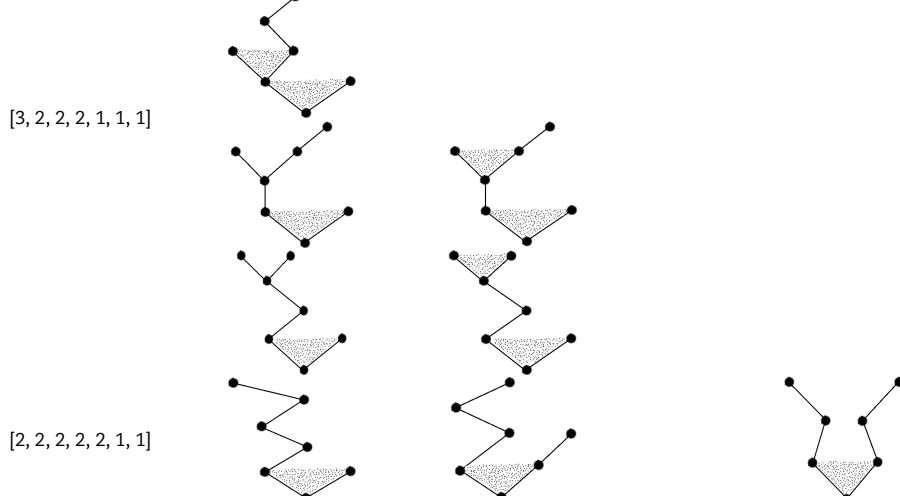
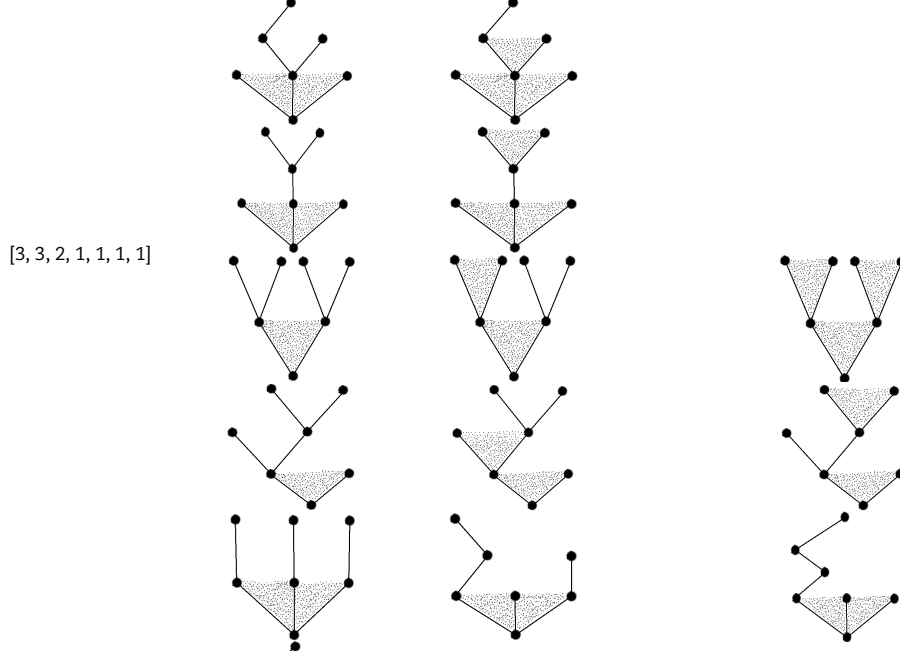
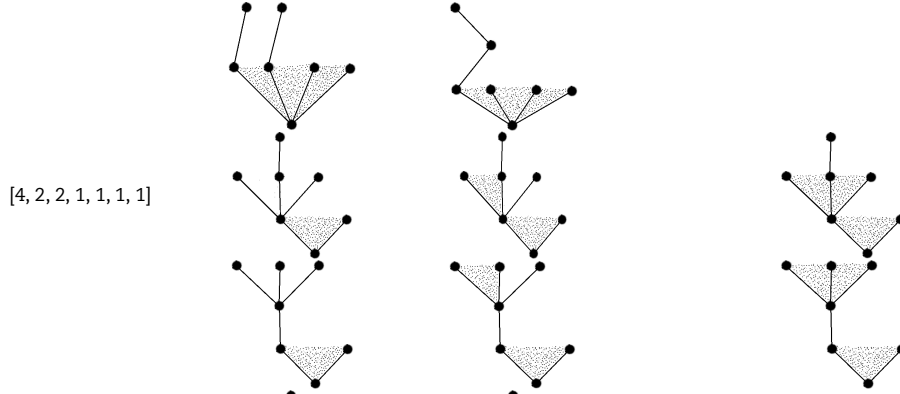
A nested-If statements MATLAB software can be used to derive the solutions to Equations (33) and (34). Five link assortments can be obtained, namely  $[2, 5, 0, 0], [3, 3, 1, 0], [4, 1, 2, 0], [4, 2, 0, 1]$ , and  $[5, 0, 1, 1]$ . An array of integers  $[d_1, d_2, d_3, \dots, d_m]$  representing the number of vertices with the same degree in ascending order is called a VDA. As an illustration, the array of vertex degrees for the link assortment  $[4, 2, 0, 1]$  is  $[4, 2, 2, 1, 1, 1, 1]$ . Families are used to classify VDAs.

- Family 1:  $[4, 3, 1, 1, 1, 1, 1], [4, 2, 2, 1, 1, 1, 1]$
- Family 2:  $[3, 3, 2, 1, 1, 1, 1], [3, 2, 2, 2, 1, 1, 1]$
- Family 3:  $[2, 2, 2, 2, 2, 1, 1]$





(a) Spanning trees resulting from the VDA [4, 3, 1, 1, 1, 1, 1].



(b) Spanning trees resulting from the VDAs [4, 2, 2, 1, 1, 1, 1], [3, 3, 2, 1, 1, 1, 1], [3, 2, 2, 2, 1, 1, 1], and [2, 2, 2, 2, 2, 1, 1].

Fig. 10. Spanning trees resulting from the five VDAs.



Table 2. VDAs of the parent graphs.

VDAs of the parent graphs
[3, 3, 3, 3, 2, 2, 2]
[4, 3, 3, 2, 2, 2, 2]
[4, 4, 2, 2, 2, 2, 2]

Figure 10(a) illustrates the spanning trees produced from the VDA [4, 3, 1, 1, 1, 1, 1]. Using the five VDAs, we counted thirty-six spanning trees, as shown in Figs. 10 (a) and (b). These spanning trees can be used to generate 3-DOF PGMs with non-fractionated 2-DOF PGTs.

Problems with determining the TV for each FC arise when trying to automate the parent graph technique [29]. The newly proposed approach, on the other hand, can quickly identify TVs from a spanning tree. Since all labeled spanning trees correspond to non-isomorphic tree topologies, it appears that geared graphs must be created from all spanning trees, followed by an isomorphic check that yields an exhaustive list of candidates

5.2. Synthesis of geared graphs

The primary process in generating geared graphs is to add geared edges to spanning trees. A geared edge can only be incident with a pair of vertices if the path connecting them contains exactly two revolute edges. There are  $n - 4$  geared edges in an  $n$ -link 3-DOF PGM graph. The number of independent loops is  $L = e_g = n - 1 - F$ . Using the following equations, every potential link combination for 3-DOF PGMs with seven links can be calculated.

$$V_2 + V_3 + V_4 + \dots + V_m = v \tag{35}$$

$$2V_2 + 3V_3 + 4V_4 + \dots + mV_m = 2e \tag{36}$$

With  $v = 7, F = 3, e = 9$ , and  $m = 7 - 3 = 4$ , we obtain from Eqs. (35) and (36)

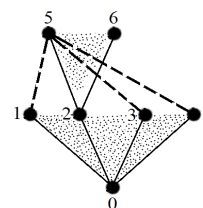
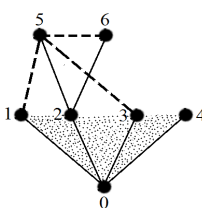
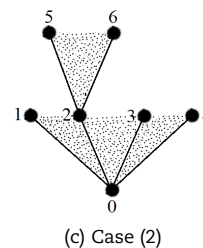
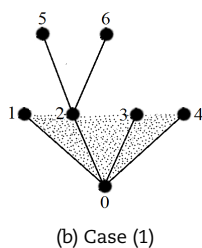
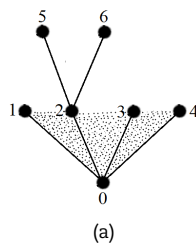
$$V_2 + V_3 + V_4 = 7 \tag{37}$$

$$2V_2 + 3V_3 + 4V_4 = 18 \tag{38}$$

Equations (37) and (38) can be solved using a MATLAB program with nested If statements. Three link assortments can be obtained, namely [3, 4, 0], [4, 2, 1], and [5, 0, 2]. The corresponding VDAs are shown in Table 2.

For the addition of geared edges, the following guidelines are applied:

- G1: It is not possible to join two vertices on the same dotted polyline using gear edges.
- G2: A geared edge can only be incident with a pair of vertices if the path linking them has exactly two revolute edges, two polylines, or a revolute edge and a polyline.
- G3: The geared graphs are guaranteed to be closed-loop graphs by imposing a minimum vertex degree of 2, i.e., by checking that the array of vertex degrees is consistent with the list of permitted vertex degrees.
- G3: Check for probable graph isomorphism for each geared graph created.
- G4: It is essential to ensure that no sub-chains are locked; in Fig. 11(f), for example, the presence of the loop created by geared edges forces the gear train to depend on particular link length dimensions to accomplish mobility or prevents obtaining valid transfer vertices.



(d) VDA=[4, 4, 3, 2, 2, 2, 1]. Violate the VDAs of the geared graph. (e) VDA=[4, 4, 3, 2, 2, 2, 1]. Violate the VDAs of the geared graph.

Fig. 11. Adding geared edges to a spanning tree and the resulting VDA.



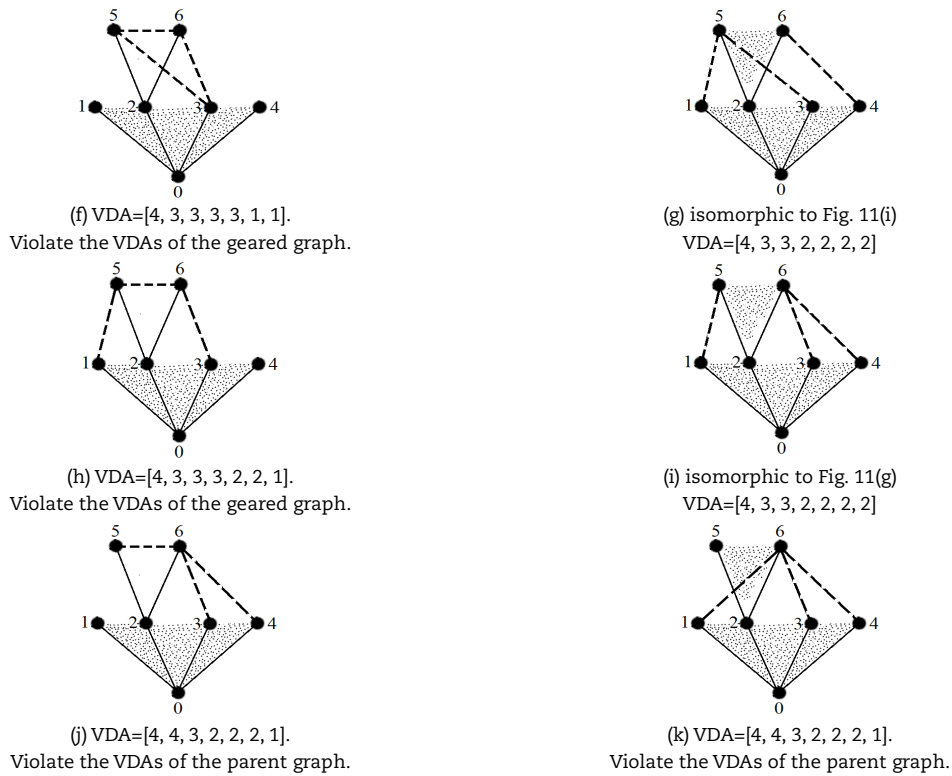


Fig. 11. Continued.

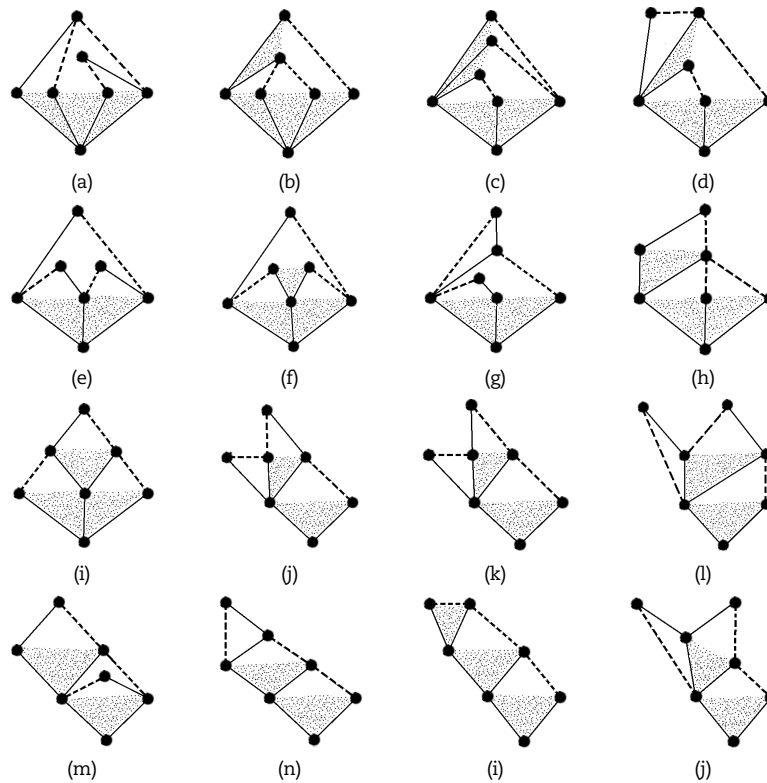


Fig. 12. The non-isomorphic geared graphs for 7-link 3-DOF PGMs.

Figure 11(a) depicts a spanning tree that will be used to illustrate the concept of adding geared edges. There are three geared edges to be added. Because the two second level vertices in Fig. 11(a), vertices 5 and 6, are incident to a common vertex, vertex 2, two possibilities exist:

**Case (1):** One geared edge joins the two second-level vertices, and the graph requires two additional geared edges to be finished. To prevent the formation of a redundant link, the first-level vertices (1, 3, and 4) should be incident by a minimum of one geared edge. Two geared edges added to three first-level vertices will result in one vertex lacking an incident-geared edge.

**Case (2):** There is no geared edge connecting the two second level vertices. The two vertices on the second level will be connected to the three vertices on the first level, which are numbered 1, 3, and 4. This will require the utilization of all three



geared edges. To avoid the creation of redundant links, each of the three first-level vertices must be linked by a single geared edge. As a result, the three geared edges can be distributed between the two second-level vertices in four different ways. The following are the distributions: (3+0), (2+1), (1+2), and (0+3). As a result of the similarities between the vertices 1, 3, and 4, two isomorphic graphs emerge from the (1+2) and (2+1) distributions, as will be discussed in the following section. As a result, the three geared edges can only be distributed among the three first-level vertices in one distinct non-isomorphic method. All of images (d), (e), (f), (h), (j), and (k) in Fig. 11 violate the VDAs of the parent graph. At this point, it is essential to check the isomorphism for all 7-link 3-DOF PGM graphs generated.

### 5.3. Isomorphism detection

Isomorphic geared graphs can be identified using the isomorphic detection approach described in section 3.3. Each graph has a unique isomorphic identification number. All the non-isomorphic graphs for 7-link 3-DOF PGMs are shown in Fig. 12. Isomorphic graphs (not shown) have the same value of isomorphic identification number.

### 5.4. Fractionated graph detection

The fractionated 2-DOF PGTs are eliminated using the fractionation identification technique. All the 7-link 3-DOF graphs with non-fractionated 2-DOF PGTs are shown in Fig. 13.

## 6. Results and Discussion

### 6.1. Results

In this work, we propose an approach for synthesizing 3-DOF PGMs (or 2-DOF PGTs). First, 3-DOF PGM-spanning trees are synthesized. All feasible link assortments are formed for a given number of links  $n$ , according to Eqs. (31) and (32). Labeled spanning trees corresponding to non-isomorphic tree topologies are constructed based on the link assortments, transfer vertices, and vertex levels. The VDAs are obtained using a nested-If statements MATLAB program and the spanning trees are built based on the fundamental characteristics of the PGT graphs. Seven-link spanning trees for the vertex degree array [4, 3, 1, 1, 1, 1, 1] are shown in Fig. 10(a), and a complete list of all 36 such trees is provided in Fig. 10(b).

Second, 3-DOF PGMs are synthesized using the labelled spanning tree atlas. From the labelled spanning trees, potential geared graphs are constructed by specifying transfer vertices and distributing geared edges. The guidelines for including geared edges and how to synthesize geared graphs from spanning trees are outlined in Section 5.2 (Synthesis of geared graphs). A nested MATLAB program was used to acquire the arrays of vertex degrees of the geared graphs. It uses if statements. Three vertex degree arrays, given in Table 2, are generated and utilized to validate the geared graphs. The geared graphs that violate the vertex degree arrays of the parent graph are deleted. Isomorphic geared graphs are identified by comparing the isomorphic identification numbers of geared graphs with the same spanning tree. It is true that geared graphs constructed from distinct spanning trees are non-isomorphic. All the non-isomorphic geared graphs for 7-link 3-DOF PGMs are shown in Fig. 12.

It is important to identify and get rid of any fractionated PGTs. Here, we introduce a straightforward new technique for identifying fractionated PGT graphs. Previous techniques relied on the rotation graphs rather than displacement graphs to detect fractionation. When the graph of a fractionated PGT is transformed into a rotation graph, the cut vertex is the one whose removal results in a larger number of components. The new method relies on the successive deletion of revolute joints with the same labeling from the geared graphs. A graph is considered to be fractionated if at least one of its resulting sub-graphs is also fractionated with a larger number of components using a single application of upper-level vertices separation. Fractionated geared graphs are identified using the reachability matrix method. Previous fractionated detection approaches, which relied on independent loop combinations, differ significantly from the proposed method. The new method works for all possible graph representations and has a straightforward algorithm. All the 7-link 3-DOF graphs with non-fractionated 6-link 2-DOF PGTs are shown in Fig. 13.

### 6.2. Causes of using rooted graph

For the graph shown in Fig. 14(a), taken from the work of Yang et al. [29] (Fig. 21(a)), we have  $v = 8$  and  $e_r = 7$ ,  $e_g = 3$ . Equation (2) gives  $F = 3(8 - 1) - 2 \times 7 - 3 = 4$ . The graph in Fig. 14(a) can be reconfigured using the vertex selection technique to become one with two separating vertices, as seen in Fig. 14. Therefore, it is a fractionated 4-DOF PGM graph. This graph model has trouble accurately modeling a PGM containing multiple joints.

Because of the above-mentioned trouble to accurately modeling a PGM containing multiple joints, the rooted graph (which corresponds to its mechanism) was used in this study. The following is an explanation of the advantages of utilizing a rooted graph representation.

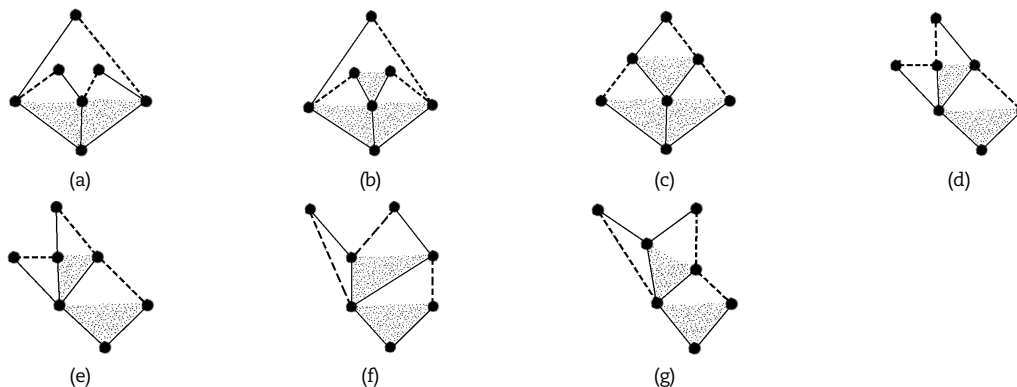


Fig. 13. The 7-link 3-DOF graphs with non-fractionated 2-DOF PGTs.



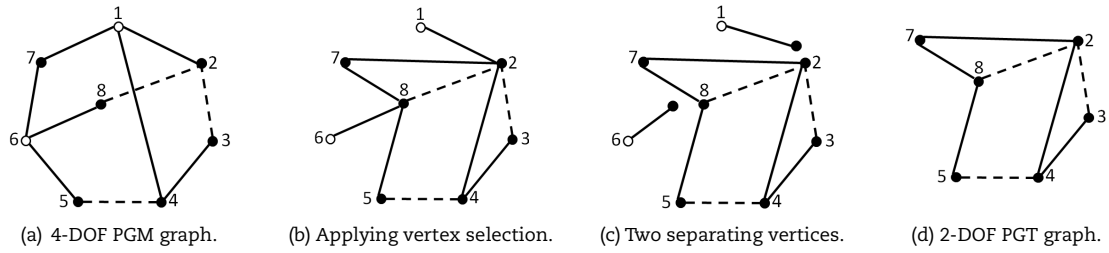


Fig. 14. Fractionation process of the graph taken from the work of Yang and Ding [29] (Fig. 21 (a)).

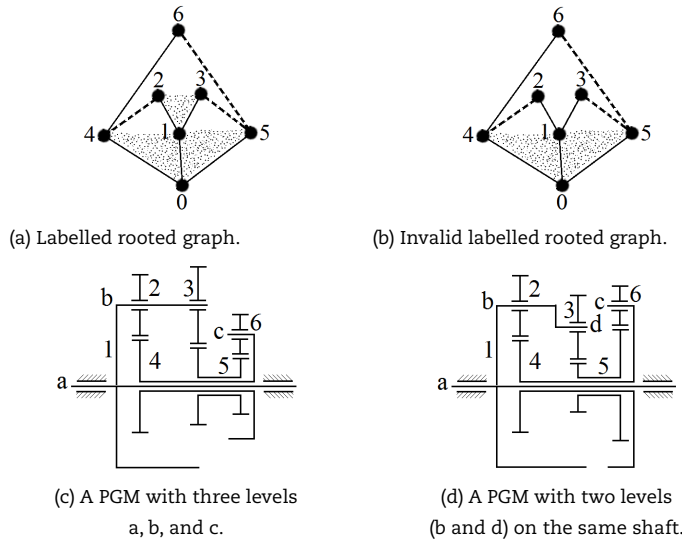


Fig. 15. Labelled graphs with distinct edge levels.

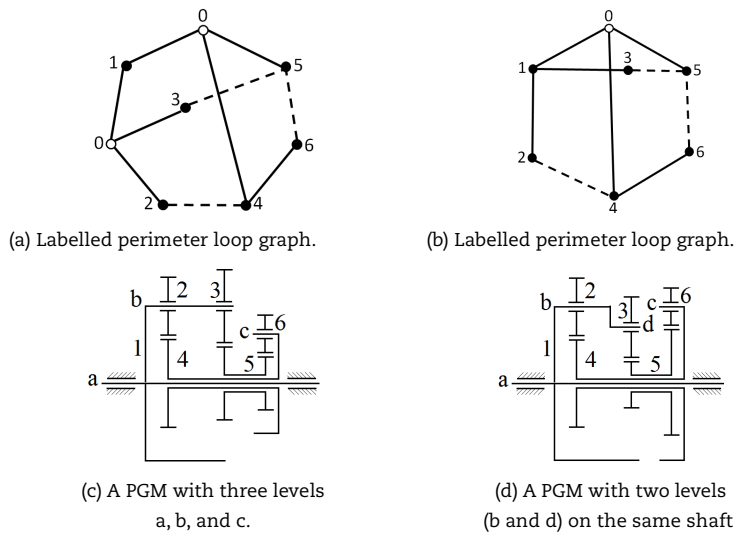


Fig. 16. Lack of correspondence between the functional diagram elements and the hollow vertex graph.

**1. Labeling the edge levels:** All revolute edges within a specific polyline region have the same level, however all other revolute edges have different levels. Therefore, labeling the edge levels is unnecessary because the edge level details are already present in the rooted graph.

In Fig. 15(a), the edges 0-1, 0-4, and 0-5 are all at the same level. Edges 1-2 and 1-3 are at the same level but differ from the preceding one, and edge 4-6 is at a different level. As a result, it is obvious that there are three distinct edge levels.

Figure 15(a) and 15(b) illustrate two isomorphic rooted graphs with the same number of vertices and edges. Moreover, the degrees of the corresponding vertices are identical. They differ only in the labeling of the edge levels. The only difference between Figs. 15(c) and 15(d) is the labeling of the edge levels; otherwise, they are structurally identical. In such circumstances, the difference is not significant enough to warrant distinguishing whether it is on one or two levels, because the lack of a geared edge causes them to be considered on the same level even though if they are on two levels. The current rooted graph representation cannot contain a gear joint between two gears rotating in different axes on the same shaft (gears 2 and 3 in both cases). Therefore, they are considered to be rotating about the same axis while maintaining the necessary representational consistency. As a result, the graph in Fig. 15(a) represents the two mechanisms, whereas Fig. 15(b) is considered to be invalid.



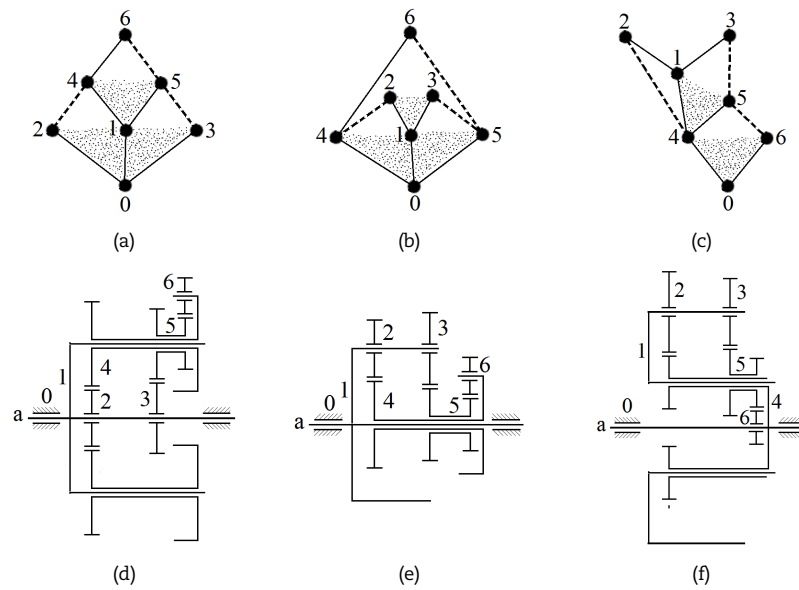


Fig. 17. Viable functional diagrams relating to three graphs.

**2. One-to-one correspondence:** There is a one-to-one correspondence between the elements of the PGM and those of the rooted graph.

PGM can be graphically represented in a number of methods. Some methods do not always have a one-to-one correspondence. When there is a correspondence between the elements of a graph and the elements of its PGM, the numerical correspondence relationships given in Table 1 hold. However, the graph representation presented by Yang and Ding [29], necessitates the addition of a hollow vertex for any set of revolute edges with the same level. Each time a hollow vertex is added, the number of vertices and the number of revolute edges is increased by one. It is presumed that Fig. 16(c) differs from Fig. 16(d) only in the labeling of the edge levels, but it actually differs in regard to the number of revolute edges and vertices. As a result, there is no correspondence between the elements of the functional schematic diagram and the hollow vertex graph. Therefore, in the perimeter loop graph representation, the inserted hollow vertex cannot be handled in the same manner as the solid vertex.

According to the details provided in the preceding paragraph, the graph in Fig. 16(b) represents the two mechanisms shown in (c) and (d). Figure 16(a), in our opinion, refers to a different mechanism, which will be discussed more below.

**3. Uniqueness:** For every possible topology of a geared graph, there is a corresponding PGM.

Each graph shown in Fig. 17 can be converted into a PGM. Using Figs. 17 (a), (b), and (c), for example, viable functional diagrams relating to these graphs are given in Figs. 17 (d), (e), and (f). Although the structure of the three PGTs is the same, their PGM structures are not.

The following structural differences can be observed, for instance, between the two PGMs depicted in Figs. 17 (d) and (e):

1. The first contains a floating carrier while the second does not.
2. In the first set, the planet gears mesh with each other, but in the second set, they do not.
3. In the first set, the revolute joints of links 1, 2, and 3 form a multiple-joint with the central shaft as its axis, but in the second set, the multiple-joint is formed by links 1, 4, and 5.
4. In the second set, each planet gear is meshed with the links that have the central shaft as their axis, but in the first set, only two of the three planet gears are meshed with the links whose axis is the central shaft.

The perimeter loop graph shown in Fig. 16 (b) corresponds to the seven-link PGM shown in Fig. 17(e). Figure 16(a) corresponds, in our reasoning, to the seven-link PGM depicted in Fig. 17(d), and will be discussed more below. PGMs like the one shown in Fig. 17(e) cannot be represented in the perimeter loop graph representation.

Although Yang and Ding [29] developed a method for synthesizing PGTs that utilized parent graphs, there is no one-to-one correspondence between the displacement graph and the PGT or PGM. Therefore, if the perimeter loop graph representation [29] is used to synthesize 3-DOF PGMs, the whole atlas of PGMs is unlikely to be achieved.

### 6.3. Causes of differing results

**1. Kinematic Inversions:** Various mechanisms are created by changing the fixed link in a kinematic chain.

One of the distinctive features of the planetary gear mechanism is the coaxial revolute joints that connect some links to the housing. When different joint axes of a PGM are chosen to be connected to the casing, there is no impact on the relative motions between any of the links in the chain. On the other hand, the motions that they make in relation to the ground could be quite different.

For example, the rooted graphs shown in Figs. 17 (a), (b), and (c) represent the three PGMs that share the same PGT in Figs. 17 (d), (e), and (f), where the common joint axes about the fixed link (0) is labeled as "a". As a result, the new method predicts all non-isomorphic inverted mechanisms. While the perimeter loop method predicts only a single graph (Fig. 16(b)). The perimeter loop representation is based on the maximal degree string loop [30], which utilizes the largest vertex degree string (VDS) and ignores the rest. As an illustration, in Fig. 16(a), the degrees of vertices 0, 1, 0, 5, 6, 4, 2, and 3 are 3, 2, 3, 2, 3, 2, and 2, respectively. The degrees of vertices 0, 5, 6, 4, 2, 0, 1, and 3 in the sequenced maximal loop are 3, 3, 2, 3, 2, 3, 2, and 2, respectively. In each case, the loop began from a different hollow vertex. The maximal degree string loop is that with the largest vertex degree string, i.e., 3323232. The perimeter loop-based technique ignores the PGM with the VDS 3232332. Figure 17(d) shows the PGM with VDS 3232332; nevertheless, Yang and Ding [29] exclude this PGM since its VDS is not maximal resulting in many PGMs being ignored.



Table 3. The results of non-fractionated geared graph synthesis.

No. of links of the PGT	No. of links of the PGM	No. of spanning trees	No. of non-isomorphic geared graphs for 3-DOF PGMs	No. of 3-DOF graphs with non-fractionated 2-DOF PGTs
6	7	24	16	7

2. **Graph Representation:** Another possible explanation is that some PGMs cannot be generated using other methods. This can be explained as follows:

The multiple-joint in PGMs represents the revolute joints of the coaxial links that rotate around an axis; it is evident that it can be formed from two or more revolute joints. The root vertex represents the fixed link (casing) around which the major axis of the coaxial links rotates. The root vertex distinguishes the PGT graph from the PGM graph. When a root is present, the PGT graph transforms into a PGM graph. Furthermore, the number of PGMs that can be generated from a PGT is sometimes equal to the number of the major axes in the PGT itself. The major axis in Fig. 17(d) is the axis around which the three links 1, 2, and 3 rotate, whereas the major axis in Fig. 17(f) is the axis around which the two links 4, and 6 rotate.

Acyclic graphs and parent graph-based methods cannot produce multiple-joint with fewer than three co-axial links [15, 16, 29]. This is due to the method used to represent PGT graphs, which states that "if a loop is entirely formed of revolute edges, the revolute edges in the loop are deleted, and the solid vertices in the loop are connected to a common hollow vertex by new revolute edges". When the number of revolute edges is less than three, it is impossible to form a loop, and thus a hollow vertex cannot exist. Therefore, acyclic graphs and parent graph-based methods cannot produce graphs with hollow vertices of degree two. Therefore, it cannot produce mechanisms like the one in Fig. 17(f). Figure 13 (d), (e), (f), and (g) show the four new PGMs with two coaxial links.

6.4. Comparison of the results

The synthesis results of 7-link 3-DOF PGMs (6-link 2-DOF PGTs) reveal the existence of seven non-fractionated mechanisms, which are four more than those reported by Tsai and Lin [24], Yang and Ding [29], and Hsu [47]. Table 3 summarizes the results of 7-link 3-DOF PGMs synthesis.

The synthesis results of Tsai and Lin [24] for non-fractionated 2-DOF PGTs with 6 links are listed in the first row of Fig. 18. The corresponding rooted graphs are shown in the second row.

The only difference between Fig. 18(b) and 18(c) is the labeling of edge 46 ( $e_{46}$ ); otherwise, they are graphically identical. Tsai and Lin [24] stated that "For six link chains, there are two blocks which have been labeled into three canonical displacement graphs." Because no geared edge connects vertices 5 and 6, it is reasonable to consider  $e_{45}$  and  $e_{46}$  to be the same labeled edges. Therefore, the graphs in Figs. 18(b) and 18(c) are equivalent to the graph in Fig. 18 (e).

Some PGM cannot be generated using the generic approach [24]. Figure 19(a), for example, is rejected by the generic approach due to the limited capabilities of its graph representation. But in fact, it is equivalent to the non-isomorphic non-fractionated graph in Fig. 19(b).

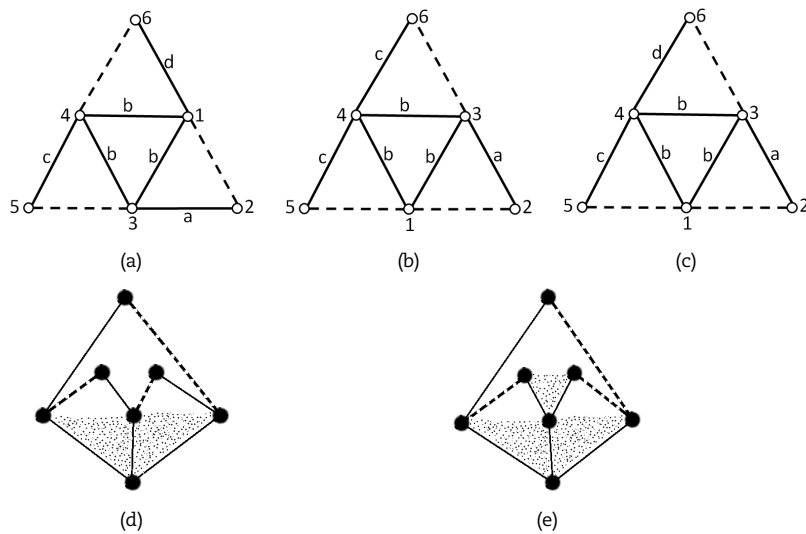


Fig. 18. (a), (b), and (c) Tsai and Lin synthesis results [24], (d) and (e) The corresponding rooted graphs.

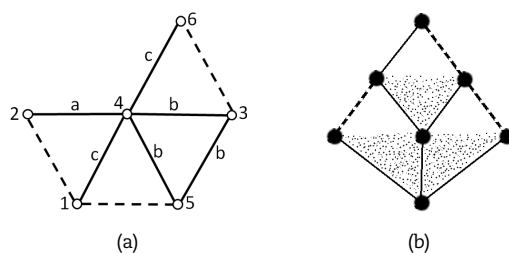


Fig. 19. (a) A rejected graph by the generic approach [24], (b) The equivalent non-isomorphic non-fractionated rooted graph.



## 7. Conclusion

Because of the troubles to accurately modeling a PGM containing multiple joints, the rooted graph (which corresponds to its mechanism) has been used in this study. The advantages of the rooted graph representation over the perimeter loop-based graph representation are outlined. There is a one-to-one correspondence between the elements of the PGM and those of the rooted graph. All revolute edges within a specific polyline region have the same level, however all other revolute edges have different levels. There is one and only one PGM for each feasible topology of a geared graph. The proposed method efficiently detects TVs using spanning trees. The method is an improvement over previous methods that were both laborious and highly automated. The creation of geared graphs involves creating non-isomorphic tree topologies from all spanning trees and conducting an isomorphic check to generate a comprehensive list of candidates. The synthesis results of 7-link 3-DOF PGMs reveal the existence of seven non-fractionated mechanisms, which are four more than those reported in the literature. The new method also accurately predicts any inverted mechanisms that are not isomorphic to each other. Unlike other approaches, which cannot build graphs with hollow vertices of degree two, the rooted graph method can. An approach based on the weighted vertex degree array and the weighted vertex-circuit matrix has been developed to find isomorphic graphs. Isomorphic geared graphs are detected by comparing the isomorphic identification numbers of geared graphs with the same spanning tree. A simple new technique for detecting fractionated PGM graphs is presented. The reachability matrix method is used to locate fractionated geared graphs. Previous fractionated detection techniques, which relied on independent loop combinations, differ significantly from the proposed method. The novel technique, which has a simple algorithm, works for all possible graph representations. The reasons why the results of this study differ from earlier studies have been highlighted and explained.

## Author Contributions

The manuscript was written through the contribution of all authors. All authors discussed the results, reviewed, and approved the final version of the manuscript.

## Acknowledgments

Not applicable.

## Conflict of Interest

The authors declared no potential conflicts of interest concerning the research, authorship, and publication of this article.

## Funding

The authors received no financial support for the research, authorship, and publication of this article.

## Data Availability Statements

The datasets generated and/or analyzed during the current study are available from the corresponding author on reasonable request.

## Nomenclature

$A$	The adjacency matrix	$J_r$	The number of revolute joints
$\tilde{A}$	The reduced adjacency matrix	$J_g$	The number geared joints
$C_v$	The vertex-circuit matrix	$L$	Number of independent loops
$[C_v]_w$	The weighted vertex-circuit matrix	$m$	The maximal degree of vertex
$c_i$	Fundamental circuit $i$	$n$	Number of Links
$D$	The vertex degree array matrix	$o$	Root or the ground vertex
$D_w$	The weighted vertex degree array	$rm(i, j)$	The $(i, j)$ element of RM
$d_i$	The degree of a vertex $i$	$v$	Number of vertices
$e$	Number of edges	$v_i$	Vertex $i$
$e_r$	The number of revolute edges	$V_2, V_3, \dots, V_m$	Number of binary, ternary... $m$ -nary vertices of geared graph
$e_g$	The number of geared edges	$[V_1, V_2, V_3, \dots, V_m]$	Link assortment array for spanning tree
$e_{ij}$	The edge between vertex $i$ and $j$	CDS	The circuit degree string
$F$	Number of degrees of Freedom	DOF	Degree of Freedom
$FCAA$	The fundamental circuit assortment array	PGT	Planetary gear train
$f_i$	The DOF in the $i^{th}$ joint	PGM	Planetary gear mechanism
$IIN$	The isomorphic identification number	RM	The reachability matrix
$I$	The identity matrix	VDA	The vertex degree array
$J$	The total number of joints	VDS	Vertex degree string

## References

- [1] Li, M., Xie, L.Y., Ding, L.J., Load sharing analysis and reliability prediction for planetary gear train of helicopter, *Mech. Mach. Theory*, 115, 2017, 97–113.
- [2] Ding, H.F., Huang, P., Zi, B., Kecskemethy, A., Automatic synthesis of kinematic structures of mechanisms and robots especially for those with complex structures, *Appl. Math. Model.*, 36, 2012, 6122–6131.
- [3] Xie, T.L., Hu, J.B., Peng, Z.X., Liu, C.W., Synthesis of seven-speed planetary gear trains for heavy-duty commercial vehicle, *Mech. Mach. Theory*, 90, 2015, 230–239.
- [4] Du, M., Yang, L., A basis for the computer-aided design of the topological structure of planetary gear trains, *Mech. Mach. Theory*, 145, 2020, 103690.
- [5] Tsai, L.W., *Mechanism design: Enumeration of Kinematic Structures According to Function*, CRC Press, 2000.
- [6] Pennestri, E., Belfiore, N.P., On Crossley's contribution to the development of graph-based algorithms for the analysis of mechanisms and gear trains, *Mech. Mach. Theory*, 89, 2015, 92–106.



- [7] Tsai, L.W., An application of the linkage characteristic polynomial to the topological synthesis of epicyclic gear train, *ASME J. Mech., Transm. Autom. Des.*, 109, 1987, 329–336.
- [8] Kim, J.U., Kwak, B.M., Application of edge permutation group to structural synthesis of epicyclic gear trains, *Mech. Mach. Theory*, 25, 1990, 563–574.
- [9] Shin, J.K., Krishnamurthy, S., Standard code technique in the enumeration of epicyclic gear trains, *Mech. Mach. Theory*, 28, 1993, 347–355.
- [10] Hsu, C.H., Lam, K.T., Yin, Y.L., Automatic synthesis of displacement graphs for planetary gear trains, *Math. Comput. Model.*, 19, 1994, 67–81.
- [11] Hsu, C.H., Hsu, J.J., An efficient methodology for the structural synthesis of geared kinematic chains, *Mech. Mach. Theory*, 32, 1997, 957–973.
- [12] Del Castillo, J.M., Enumeration of 1-DOF planetary gear train graphs based on functional constraints, *ASME J. Mech. Des.*, 124, 2002, 723–732.
- [13] Rao, Y.V.D., Rao, A.C., Generation of epicyclic gear trains of one degree of freedom, *ASME J. Mech. Des.*, 130, 2008, 052604.
- [14] Kamesh, V.V., Rao, K.M., Rao, A.B.S., Detection of degenerate structure in single degree-of-freedom planetary gear trains, *ASME J. Mech. Des.*, 139, 2017, 083302.
- [15] Yang, W.J., Ding, H.F., Zi, B., Zhang, D., New graph representation for planetary gear trains, *ASME J. Mech. Des.*, 140, 2018, 012303.
- [16] Yang, W.J., Ding, H.F., The complete set of one-degree-of-freedom planetary gear trains with up to nine links, *ASME J. Mech. Des.*, 141, 2019, 043301.
- [17] Shanmukhasundaram, V.R., Rao, Y.V.D., Regalla, S.P., Enumeration of displacement graphs of epicyclic gear train from a given rotation graph using concept of building of kinematic units, *Mech. Mach. Theory*, 134, 2019, 393–424.
- [18] Shanmukhasundaram, V.R., Rao, Y.V.D., Regalla, S.P., Algorithms for detection of degenerate structure in epicyclic gear trains using graph theory, *J. Braz. Soc. Mech. Sci. Eng.*, 41, 2019, 496.
- [19] Buchsbaum, F., Freudenstein F., Synthesis of kinematic structure of geared kinematic chains and other mechanisms, *J. Mech.*, 5, 1970, 357–392.
- [20] Freudenstein, F., An application of Boolean algebra to the motion of epicyclic drives, *J. Eng. Ind.*, 93, 1971, 176–182.
- [21] Ravisankar, R., Mruthyunjaya, T., Computerized synthesis of the structure of geared kinematic chains, *Mech. Mach. Theory*, 20, 1985, 367–387.
- [22] Cui, R., Ye, Z., Sun, L., Zheng, G., Wu, C., Synthesis method for planetary gear trains without using rotation graphs, *Proc. IMechE Part C: J. Mech. Eng. Sci.*, 236, 2022, 972–983.
- [23] Kamesh, V.V., Mallikarjuna Rao, K., Rao, S., et al., Topological synthesis of epicyclic gear trains using vertex incidence polynomial, *J. Mech. Des.*, 139, 2017, 139.
- [24] Tsai, L.-W., Lin, C.-C., The creation of nonfractionated, two-degree-of-freedom epicyclic gear trains, *J. Mech. Transm. Autom.*, 111, 1989, 524–529.
- [25] Shanmukhasundaram, V.R., Rao, Y.V.D., Regalla, S.P., Varadaraju, D., Pennestrì, E., *Structural Synthesis and Classification of Epicyclic Gear Trains: An Acyclic Graph-Based Approach*, In: Rao, Y.V.D., Amarnath, C., Regalla, S.P., Javed, A., Singh, K.K. (eds) *Advances in Industrial Machines and Mechanisms. Lecture Notes in Mechanical Engineering*, Springer, Singapore, 2021.
- [26] Nafeh, H.A., Esmail, E.L., Abdali, S.H., Automatic Structural Synthesis of Planetary Geared Mechanisms using Graph Theory, *J. Appl. Comput. Mech.*, 9, 2023, 384–403.
- [27] Shanmukhasundaram, V.R., Rao, Y.V.D., Regalla, S.P., *Review of structural synthesis algorithms for epicyclic gear trains*, In: D. Sen, S. Mohan, G. Ananthasuresh (eds), *Mechanism and Machine Science. Lecture Notes in Mechanical Engineering*, Springer, Singapore, 2021.
- [28] Xue, H.L., Liu, G., Yang, X.H., A review of graph theory application research in gears, *Proc. IMechE Part C: J. Mech. Eng. Sci.*, 230, 2016, 1697–1714.
- [29] Yang, W.J., Ding, H.F., Kecskeméthy, A., Automatic Structural Synthesis of Non-Fractionated 2-DOF Planetary Gear Trains, *Mech. Mach. Theory*, 155, 2021, 104125.
- [30] Yang, W., Ding, H., The Perimeter Loop-Based Method for the Automatic Isomorphism Detection in Planetary Gear Trains, *J. Mech. Design*, 140, 2018, 1–10.
- [31] Yang, W., Ding, H., Automatic detection of degenerate planetary gear trains with different degree of freedoms, *Appl. Math. Model.*, 64, 2018, 320–332.
- [32] Rai, R.K., Punjabi, S., A new algorithm of links labelling for the isomorphism detection of various kinematic chains using binary code, *Mech. Mach. Theory*, 131, 2019, 1–32.
- [33] Yi, H.J., Wang, J.P., Hu, Y.L., Yang, P., Mechanism isomorphism identification based on artificial fish swarm algorithm, *Proc. IMechE Part C: J. Mech. Eng. Sci.*, 235, 2021, 5421–5433.
- [34] Zou, Y.H., He, P., An algorithm for identifying the isomorphism of planar multiple joint and gear train kinematic chains, *Math. Probl. Eng.*, 2016, 5310582.
- [35] Huang, P., Liu, T.T., Ding, H.F., Zhao, Y.Q., Isomorphism identification algorithm and database generation for planar 2–6 DOFs fractionated kinematic chains combined by two or three non-fractionated kinematic chains, *Mech. Mach. Theory*, 166, 2021, 104520.
- [36] He, L.Y., Liu, F.X., Sun, L., Wu, C.Y., Isomorphic identification for kinematic chains using variable high-order adjacency link values, *J. Mech. Sci. Technol.*, 33, 2019, 4899–4907.
- [37] Rai, R.K., Punjabi, S., Kinematic chains isomorphism identification using link connectivity number and entropy neglecting tolerance and clearance, *Mech. Mach. Theory*, 123, 2018, 40–65.
- [38] Kamesh, V.V., Rao, K.M., Rao, A.B.S., An innovative approach to detect isomorphism in planar and geared kinematic chains using graph theory, *J. Mech. Des.*, 139, 2017, 122301.
- [39] Hsu, C.-H., Displacement isomorphism of planetary gear trains, *Mech. Mach. Theory*, 29, 1994, 513–523.
- [40] Shin, J.K., Krishnamurthy, S., Standard code technique in the enumeration of epicyclic gear trains, *Mech. Mach. Theory*, 28, 1993, 347–355.
- [41] Mruthyunjaya, T.S., Raghavan, M.R., Structural analysis of kinematic chains and mechanisms based on matrix representation, *ASME J. Mech. Des.*, 101, 1979, 488–494.
- [42] Ravisankar, R., Mruthyunjaya, T.S., Computerized synthesis of the structure of geared kinematic chains, *Mech. Mach. Theory*, 20, 1985, 367–387.
- [43] Hsu, C.H., Lam, K.T., A new graph representation for the automatic kinematic analysis of planetary spur-gear trains, *ASME J. Mech. Des.*, 114, 1992, 196–200.
- [44] Hsu, C.H., A graph representation for the structural synthesis of geared kinematic chains, *J. Franklin Inst.*, 330, 1993, 913–927.
- [45] Salgado, D.R., Castillo, J.M.D., A method for detecting degenerate structures in planetary gear trains, *Mech. Mach. Theory*, 40, 2005, 948–962.
- [46] Vijayarathi, A., Anjaneyulu, G.S.G.N., Wiener Index of a graph and chemical applications, *Int. J. Chem. Tech. Res.*, 5, 2013, 1847–1853.
- [47] Hsu, C.H., Synthesis of kinematic structure of planetary gear trains by admissible graph method, *J. Frankl. Inst.*, 330, 1993, 913–927.

## ORCID iD

Sajad H. Abdali  <https://orcid.org/0009-0007-5658-6126>

Essam L. Esmail  <https://orcid.org/0000-0002-2507-786X>



© 2023 Shahid Chamran University of Ahvaz, Ahvaz, Iran. This article is an open access article distributed under the terms and conditions of the Creative Commons Attribution-NonCommercial 4.0 International (CC BY-NC 4.0 license) (<http://creativecommons.org/licenses/by-nc/4.0/>).

**How to cite this article:** Abdali S.H., Esmail E.L. The Structural Synthesis of Non-fractionated, Three-degree-of-freedom Planetary Gear Mechanisms, *J. Appl. Comput. Mech.*, 10(1), 2024, 205–223. <https://doi.org/10.22055/jacm.2023.44563.4240>

**Publisher's Note** Shahid Chamran University of Ahvaz remains neutral with regard to jurisdictional claims in published maps and institutional affiliations.

